Lake ice [in "State of the Climate in 2020"]

Book or Report Section

Published Version

It is advisable to refer to the publisher's version if you intend to cite from the work. See Guidance on citing.

To link to this article DOI: http://dx.doi.org/10.1175/2021BAMSStateoftheClimate.1

Publisher: Bulletin of the American Meteorological Society

www.reading.ac.uk/centaur

CentAUR

Central Archive at the University of Reading

In Sweden, all three glaciers reporting had a negative balance averaging −320 mm. In Norway, the eight reporting glaciers had a positive average mass balance of +365 mm in 2020. All 36 Norway glaciers surveyed in 2019 were retreating (Andreasson 2020). On Svalbard, the mean loss of three glaciers in 2020 was −1485 mm. Iceland completed surveys of nine glaciers, of which eight had negative balances with a mean mass balance of −442 mm.

In Alaska and Washington, all 14 glaciers observed in 2020 had a negative mass balance averaging −722 mm. This was significantly larger than the long-term average of four United States Geological Survey benchmark glaciers, which had a cumulative mass loss since the mid-twentieth century that averaged from −580 to −300 mm yr^{-1} (O'Neel et. al. 2019).

In South America, 2020 mass balance data were reported from two glaciers in Chile, one in Ecuador, and one in Argentina; all were negative with a mean of −1056 mm. This was greater than the 2000–18 average loss observed in the Andes of −720 ± 220 mm yr^{-1} (Dussaillant et. al. 2019).

In Kyrgyzstan and Kazakhstan, nine glaciers in the Tien Shan Range had near
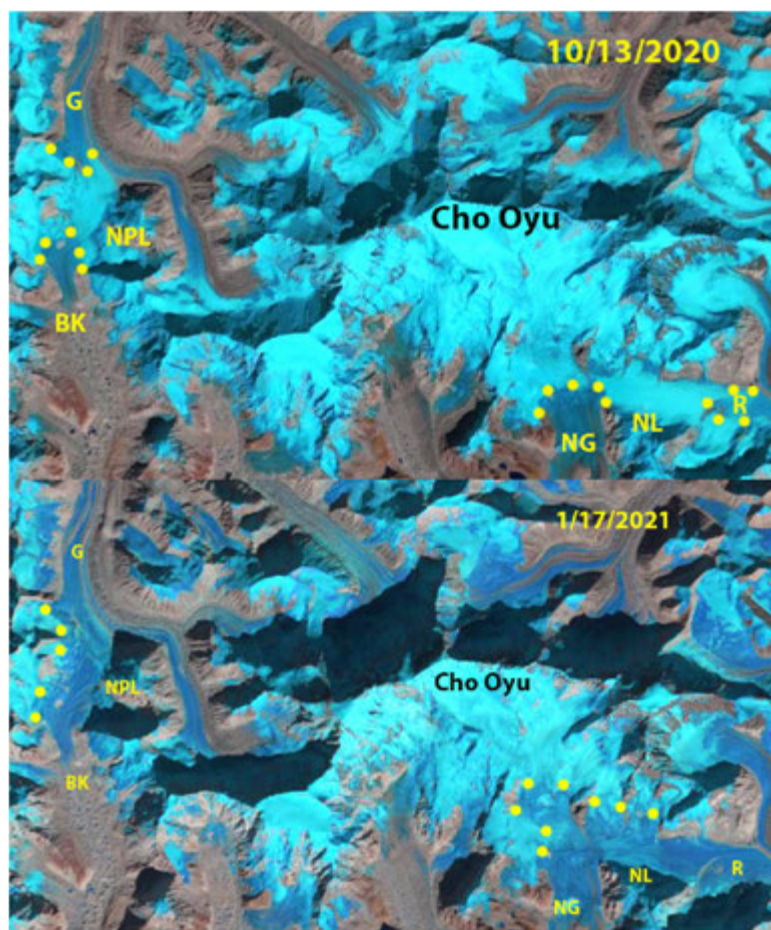

Fig. 2.15. LandSat imagery of Nangpa La (NPL-5806 m) and Nup La (NL-5850 m) 25–50 km west of Mount Everest, indicating the rise of the snow line from 13 Oct 2020 to 17 Jan 2021, leaving Nangpa La at the crest of the Gyabarg (G) and Bhote Koshi Glacier (BK) snow free. Nup La at the crest of Rongbuk (R) and Ngozumpa Glacier (NG) is also snow free on 17 Jan 2021.

equilibrium balances. In the Himalayas, the two reporting reference glaciers had negative balances averaging −487 mm. King et al. (2019) identified that in the Mount Everest region mass loss has increased each of the last 6 decades. In 2020, the post-monsoon season and early winter were warm and dry in the Himalayas, leading to the ablation season extending into January with the snow line retreating over 100 m from October into January (Fig. 2.15; Patel 2021). This raises the question, when does the ablation season end in the region in our warmer climate?

The WGMS record of mass balance and terminus behavior (WGMS 2017, 2018) provides a global index for alpine glacier behavior. Glacier mass balance is the difference between accumulation and ablation, reported here in mm of water equivalent (mm w.e.).

4) Lake ice—S. Sharma and R. I. Woolway

In the 2019/20 winter, lake ice phenology (the timing of ice-on and ice-off) across the NH (calculated from Copernicus Climate Change Service [C3S] ERA5 [Hersbach et al. 2020]) continued to experience later ice-on dates, earlier ice-off dates, and shorter seasonal ice continuing the pattern seen over 1980–2020 (Magnuson et al. 2000; Benson et al. 2012; Woolway et al. 2020). The hemispheric average for ice-on was 1.5 days later decade^{-1} and ice-off was 1.5 days earlier per decade^{-1}. In line with these calculated changes in ice phenology, the data suggest that the duration of lake ice cover was shortening at an average rate of 3 days decade^{-1}, albeit with considerable inter-annual variability ($R^2 = 0.44$). Relative to the 1981–2010 base period, NH lakes froze,

on average, 3 days later and thawed 5.5 days earlier during the 2019/20 winter season (Fig. 2.16). By ranking these ice phenology metrics according to the earliest and latest days in which they occurred since 1979/80 (the years in which these records began) we calculated that, in 2019/20, the hemispheric average ice-on was the eighth latest on record and ice-off was the third earliest. Relative to the 1981–2010 average, lake ice duration in 2019/20 was 8.5 days shorter across the NH. This was the third-shortest ice cover season since 1979/80. The regional variations in ice duration were consistent with the NH cold season (November–April) average surface air temperature anomalies (relative to 1981–2010) in 2019/20, similar to previous studies (Sharma and Woolway 2020). Most notably, some regions in North America, such as Canada, experienced below-average air temperatures, which resulted in longer-than-average ice duration. Conversely, many regions in Eurasia experienced warmer-than-average conditions that resulted in shorter-than-average ice duration (Figs. 2.16c,d).
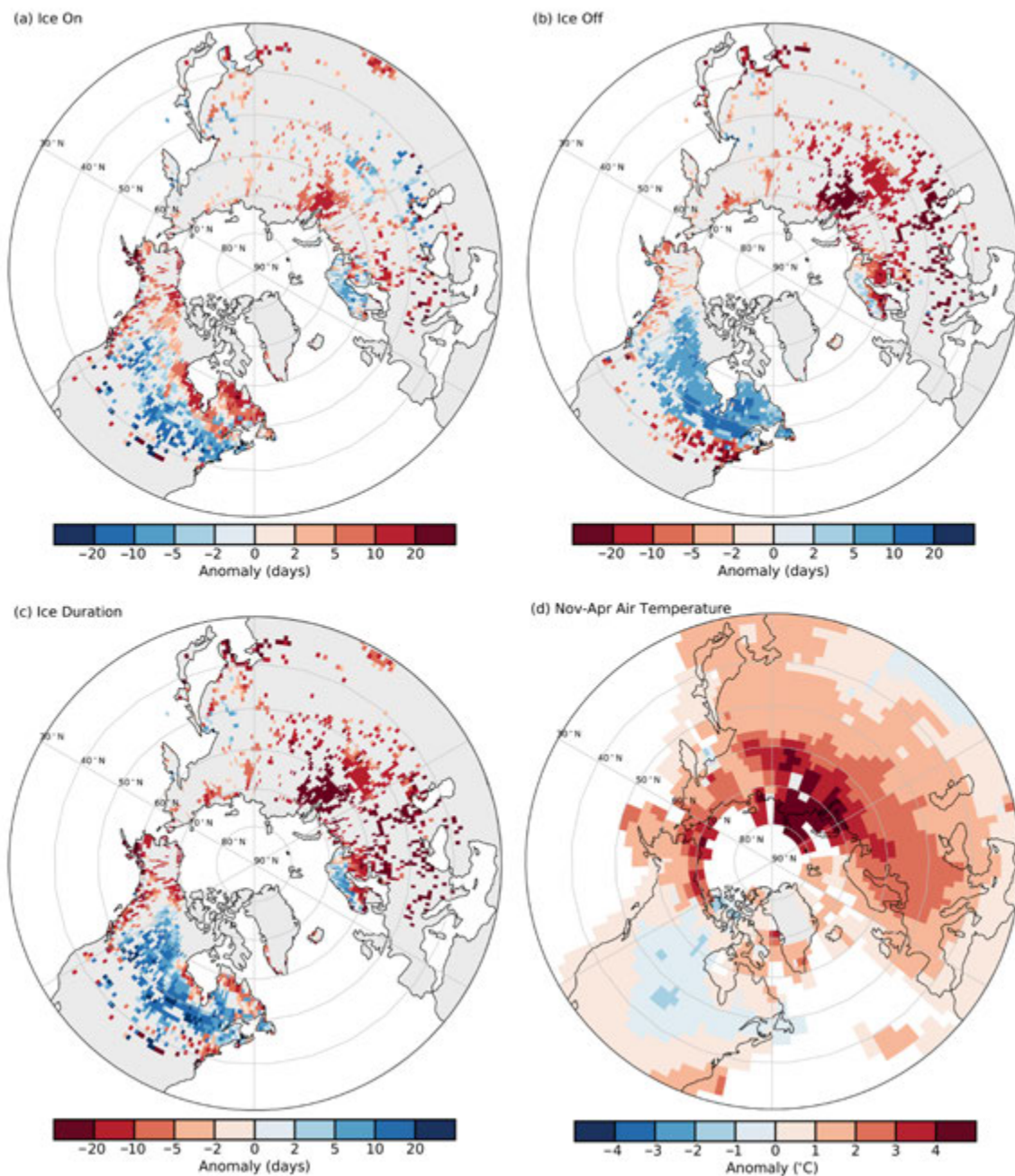
Fig. 2.16. Anomalies (days) in 2020 in (a) ice on, (b) ice off, and (c) ice duration for lakes across the NH, and (d) surface air temperature anomalies (°C) for the NH cold-season (Nov–Apr average), the time of year in which lakes typically freeze. The base period is 1981–2010. (Sources: ERA5, GISTEMP.)

In situ ice phenological records from 20 monitored lakes, situated mostly in Finland, the United States, Russia, and Canada, reveal that ice-on was 15 days later, ice-off was 11 days earlier, and there were 27 fewer days of ice cover over the winter season in 2020, on average, relative to 1981–2010 (Fig. 2.17). Lakes in Finland experienced remarkably warm conditions such that ice-on was 29 days later, ice-off was 13 days earlier, and ice duration was 42 days shorter. Typically, these Finnish lakes freeze in early December. However, during the 2020 winter, some of these same lakes froze as late as February (e.g., Lakes Nasijarvi and Visuvesi). Lakes in North America also experienced a warmer winter in 2020, with 16 fewer days of ice cover on average. Ice cover was especially anomalously low in the Finger Lakes region of New York state. For example, ice-on was 26 days later, ice-off was 16 days earlier, and ice duration was 43 days shorter for Cazenovia Lake. The winter of 2020 generally followed the long-term warming trend of 11 fewer days of ice cover for the 20 in situ lakes, on average.

In 2020, the Laurentian Great Lakes had substantially less ice cover, consistent with a warmer winter in the region. On average, the Laurentian Great Lakes had 33.9% less maximal ice coverage relative to 1981–2010. The smallest and most southern lake, Lake Erie, had the highest anomaly with a 65.4% reduction in ice coverage. Maximal ice coverage decreased by 38.1% in Lake Superior and 30.8% in Lake Huron, the two largest and most northern Great Lakes (Fig. 2.18).

To estimate the timing of ice-on and ice-off and, ultimately, the duration of winter ice cover across NH lakes, ice simulations from the ECMWFs ERA5 reanalysis product (Hersbach et al. 2020) were analyzed. Here, ice cover metrics were only calculated for pixels where lakes occupied greater than 1% of the land surface area. Lake ice conditions in 2020 were given as anomalies, calculated relative to the 1981–2010 average.
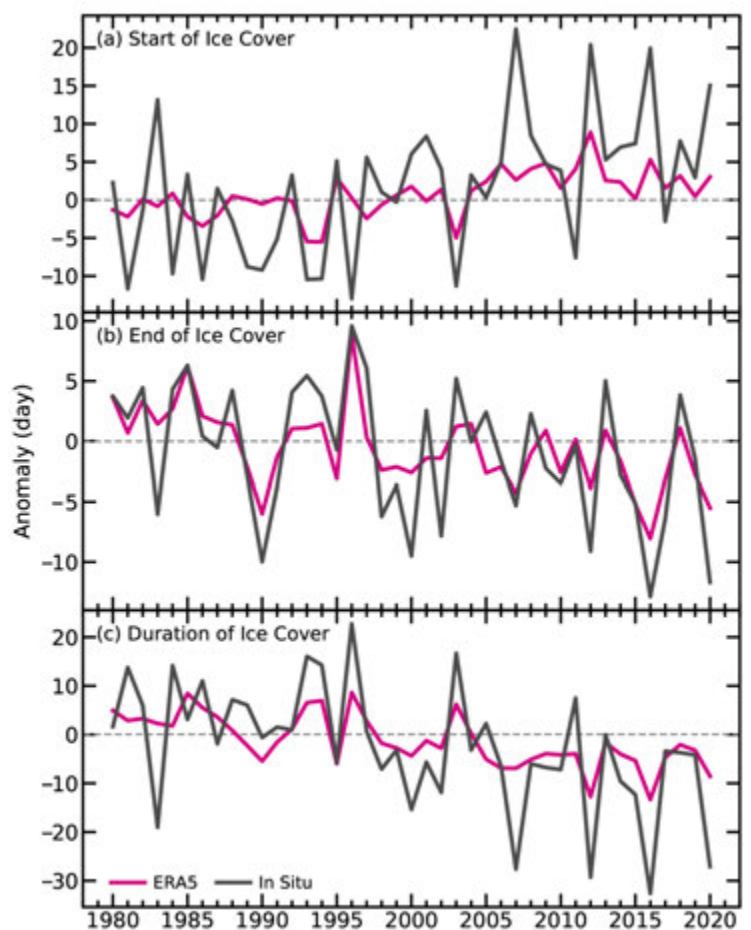

Fig. 2.17. (a) Lake ice on, (b) ice off, and (c) ice duration anomalies from 1980 to 2020 derived from in situ observations and ERA5. Base period is 1981–2010. In situ observations of ice on, ice off, and ice duration are derived from nine lakes monitored in Finland, one lake in Russia, nine lakes in the United States, and one lake in Canada.
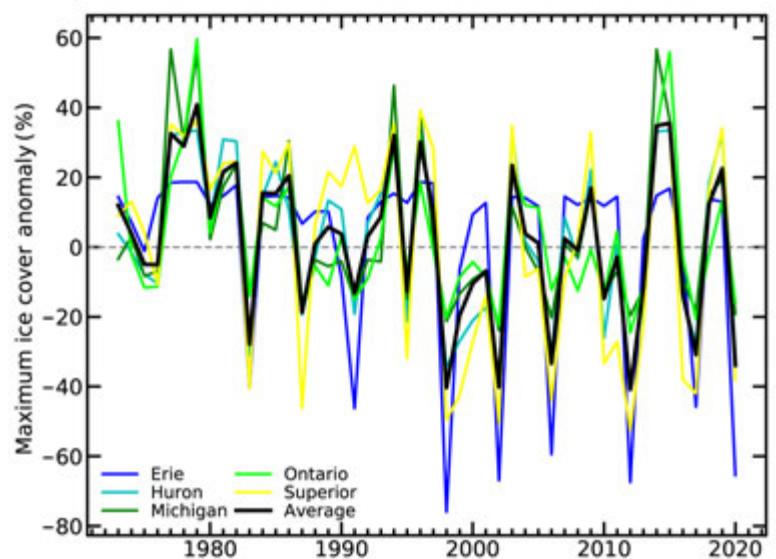

Fig. 2.18. Anomalies in Great Lakes maximum ice cover extent (%) for 1973–2020 (base period is 1981–2010). The black line shows the average anomaly for all of the Great Lakes, whereas the other lines show individual lakes (Erie, Michigan, Superior, Ontario, Huron).

Long-term in situ observations of ice-on, ice-off, and ice duration data were obtained for nine lakes in Finland, one lake in Russia, nine lakes in the United States, and one lake in Canada (Benson et al. 2000). Further, annual maximum ice cover (%) data for each of the Laurentian Great Lakes from 1973–2020 was obtained from the Great Lakes Environmental Research Laboratory. A combination of composite ice charts and observations from satellites, ships, and aircraft were used to quantify the maximum amount of ice coverage observed over the winter season in the Great Lakes (https://www.glerl.noaa.gov/data/ice/).

Surface air temperature data for the NH cold season (November–April average) were downloaded from the NASA GISS surface temperature analysis (Lenssen et al. 2019).

d. Hydrological cycle

1) Surface humidity—K. M. Willett, A. Vance, A. Simmons, M. Bosilovich, D. I. Berry, and D. Lavers

During 2020, the land surface specific humidity (q_{land})—a measure of atmospheric water vapor—remained well above average (0.14 to 0.36 g kg^{-1}), while relative humidity (RH_{land})—a measure of saturation—remained well below average (–1.28 to –0.68 %rh). Over oceans, q_{ocean} was a record high (0.23 to 0.41 g kg^{-1}) but RH_{ocean} was close to the 1981–2010 average (–0.14 to 0.13 %rh). Although the various estimates broadly agree there are differences in magnitudes and rankings (Fig. 2.19). In situ-based HadISDH and reanalyses MERRA-2 and JRA-55 show 2020 q_{land} as moister than 2019, ranking third, first, and fourth, respectively, within their records. ERA5 reanalysis shows 2020 tied with 2019, as sixth moistest on record. JRA-55 and HadISDH RH_{land} were also more saturated in 2020 but still low (third and fifth, respectively). ERA5 RH_{land} was slightly more arid than 2019, making it a record low for the second consecutive year. Over ocean, q_{ocean} was a record moist year by a large margin for HadISDH and ERA5. MERRA-2 and JRA-55 ranked q_{ocean} second and close to 2019. RH_{ocean} was more saturated in HadISDH and JRA-55 while marginally more arid in ERA5.

Taking HadISDH uncertainty into account, these rankings are less clear, but the 2020 q_{ocean} record lies outside the uncertainty range for all other years. HadISDH and ERA5 differ in input data, coverage, and processing, especially over ocean where no ship humidity data are assimilated (Simmons et al. 2021). The 2-sigma uncertainty for HadISDH broadly encompasses the ERA5 ocean values but not ERA5 land.

Surface humidity is driven by temperature and circulation patterns. The high q_{land} and record high q_{ocean} concur with the record/near-record high temperatures (section 2b1). Despite relatively neutral El Niño–Southern Oscillation (ENSO) conditions evolving to moderate La Niña conditions (section 4b), the q_{ocean} peak surpasses those of strong El Niño events (e.g., 1998, 2010, 2015–16); and the q_{land} peak is comparable for all datasets apart from ERA5.

Despite 2020 rankings differences, there is good agreement across estimates in long-term trends of increased q and decreased RH (Table 2.5). On average, the warmer air contains more water vapor, but not as much as it could, given its temperature. So, the air has become less saturated, even over oceans; ERA5, JRA-55, and HadISDH show small RH_{ocean} decreases. This is surprising given that several climate model studies show negligible or small increases in future RH_{ocean} (Held and Soden 2006; Schneider et al. 2010; Byrne and O'Gorman 2013, 2016, 2018).

HadISDH is affected by instrument and recording errors and biases along with changes in observation density, frequency, and precision (Willett et al. 2013, 2014, 2020). Reanalyses contain model and data biases and temporally changing data assimilation streams (Gelaro et al. 2017; Hersbach et al. 2020; Simmons et al. 2021). Unlike reanalyses, HadISDH is spatially incomplete, especially over the Southern Hemisphere oceans and many dry regions (where fewer people live and hence fewer weather stations). Spatially matching ERA5 to HadISDH slightly improves agreement (Fig. 2.19; Table 2.5). Over land, HadISDH reflects the well-observed regions and, hence, regions that are generally well constrained by observations in the reanalyses. Over oceans, ERA5 does not assimilate ship humidity or air temperature observations and thus poorer observational coverage has no effect, but various changes in satellite contributions do. Comparing trends over just the